Experimental Demonstration of an All-Optical Routing Node for Multihop Wavelength Routed Networks

M. Shell, *Student Member, IEEE*, M. D. Vaughn, A. Wang, D. J. Blumenthal, *Member, IEEE*, P.-J. Rigole, and S. Nilsson

***Abstract*— The experimental demonstration of an all-optical routing node for multihop packet wavelength routed networks is described. Packets are routed in real time between three space ports and five wavelengths using subcarrier multiplexed encoded headers. Fast wavelength conversion over 40 nm is achieved using a novel four section tunable semiconductor laser and a semiconductor optical amplifier. Simultaneous wavelength conversion of the baseband payload and subcarrier multiplexed header is also demonstrated.**

WAVELENGTH routed multihop all-optical networks have been proposed for scalable data-rate and format independent transport layers [1]. For a packet based network, the interface nodes must process headers and either switch packets to a local host or forward them to another node. The forwarding operation involves packet-rate wavelength conversion and switching to an outgoing network link.

In this letter, we describe the experimental demonstration of an all-optical packet routing node designed for a WDM multihop network with an arrayed-waveguide router as the interconnection fabric [2]. The node performs fast wavelength translation between five wavelengths and provides space switching between an input port, a local node, and an output port connected to a waveguide routed structure. Subcarrier header multiplexing is used to simplify header extraction and recovery [3]–[5]. We also demonstrate simultaneous wavelength conversion of subcarrier multiplexed (SCM) packet headers with baseband payload using cross gain saturation in a semiconductor optical amplifier [6]. With this approach, the destination tag can remain with the packet through multiple all-optical hops. Wavelength conversion over 40 nm is achieved by rapid tuning (2 ns) of a four-section vertical grating assisted codirectional coupler laser with grating distributed Bragg reflector [7].

The node consists of a network interface unit (NIU) and a local host. The NIU is responsible for routing incoming packets to the host or back out to the wavelength routed network. The local host can transmit/receive both baseband data and optical subcarrier multiplexed (OSCM) header information. Packets are generated by modulating an optical source with a digital baseband payload that is electrically combined with a RF multiplexed digital header. The payload and header are transmitted in parallel within a predefined cell boundary. After packets enter a node, a fraction of the optical power is tapped for header detection/recovery. Header recovery is achieved by postdetection electronic filtering of the subcarrier and coherent detection with a local oscillator [3]. The recovered header is digitally processed using a routing table/algorithm that maps the final destination address to a space/wavelength pair associated with the present node. When a packet is forwarded to another node, the local switch modulator is set to the closed state, the packet is passed through a wavelength converter and the remote switch modulator is set to the open state. Packets destined for the local host are passed through the local switch modulator and the remote switch modulator is set to the closed state to prevent unwanted signals from the wavelength converter from entering the network.

Wavelength conversion is achieved by combining a fast, wide bandwidth tunable laser [7] with cross-gain saturation in a traveling wave semiconductor optical amplifier (SOA). Following header processing, the tunable laser is switched to the desired wavelength using a digital to analog current converter and the tunable laser output is co-injected with the packet into the SOA. This conversion is synchronized with the outgoing packet using an optical delay line. The tunable laser is switched to the desired wavelength for the cell duration equal to the packet duration plus guard bands. Wavelength transitions to prevent intermediate wavelengths from entering the network.

The experimental transmitter, packet structure, and routing node are shown in Fig. 1. Individual cell frames are 1.234 μs in duration with a 90-ns guard band at each end. Each packet contains a 103.7-Mbps 32-b header multiplexed on a 3.9-GHz subcarrier and a 512-b payload at 622-Mbps baseband. Source and destination addresses are coded in every header to verify correct routing operation. Approximately 10% of the optical power is tapped from the incoming signal at the node input and the detected signal is mixed with a 3.9-GHz LO followed by a 100-MHz low-pass filter. The recovered digital header is parallelized and processed by a fast ECL routing processor that outputs one bit for two possible modulator states

Manuscript received April 17, 1996; revised June 25, 1996. This work was supported by an NSF National Young Investigator Award 9 457 148 and the NUTEK Competence Center in Photonics at the Royal Institute of Technology.

M. Shell, M. D. Vaughn, A. Wang, and D. J. Blumenthal are with the Microelectronics Research Center, School of Electrical and Computer Engineering, Georgia Institute of Technology, Atlanta, GA 30332-0250 USA.

P.-J. Rigole and S. Nilsson are with the Laboratory of Photonics and Microwave Engineering, Department of Electronics, Royal Institute of Technology, Electrum 229, S-16440, Kista, Sweden.

Publisher Item Identifier S 1041-1135(96)07411-3.

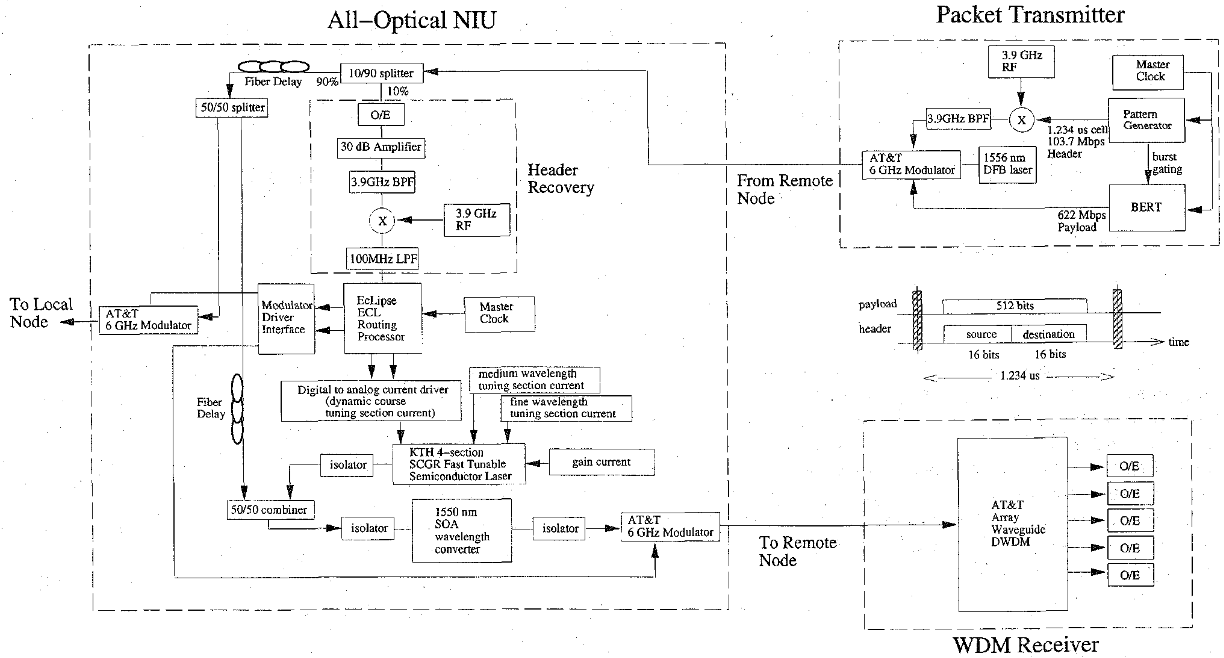

Fig. 1. Network node architecture includes network interface unit (NIU), local host, and baseband/optical-subcarrier-multiplexed transmitter/receiver.

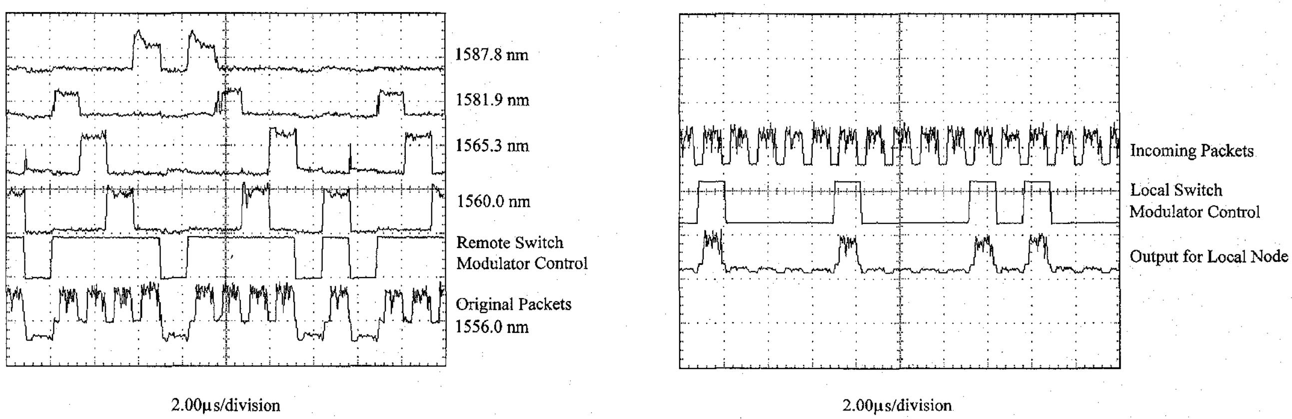

(a) (b)

Fig. 2. (a) Remote port routing function: Traces 1–4 are wavelength converted and switched packets, Trace 5 is remote modulator control signal, Trace 6 is monitor of 512-b payloads at original wavelengths. (b) Local port routing function: upper trace is input packets, middle trace is modulator control, lower trace is local port packets.

(local or remote) and two bits for four possible wavelengths. The binary wavelength information is converted to one of four current levels using a fast D/A converting circuit with subnanosecond risetime. The D/A converter drives the course tuning section of a four-section tunable laser [7] to select one of four wavelengths (1587.8 nm, 1581.9 nm, 1565.3 nm, and 1560 nm). The SOA is a 1550 nm bulk buried heterostructure semiconductor optical amplifier.

Demonstration of space-wavelength routing is shown in Fig. 2(a) and (b). Fig. 2(a) illustrates wavelength conversion and switching based on the header. The four wavelength converted channels at the remote output are shown in traces 1–4. Trace 5 is the remote switch modulator state where a low indicates a blocked output. The lower trace is 512 bit payloads at the original input wavelength. The payloads cannot be resolved in Fig. 2 because of the time scale of the trace and the low modulation depth of the payload after conversion, however, the payload bits are observable in Fig. 3(a).

Two important features to note in Fig. 2(a) are the spikes in the 1565.3 nm output and the effective broadening of packets after wavelength conversion. The spikes result from a misalignment between the wavelength converter and the remote switch modulator and are also due to the choice of setting the tunable laser to 1565.3 nm as the default wavelength when the packet is destined for the local node and no wavelength conversion is required. Misalignment between the time it takes to settle to the default wavelength and to close the remote switch modulator results in a momentary leakage of 1565.3 nm light into the guard band interval. This effect is most pronounced when tuning from 1560 nm to 1565.3

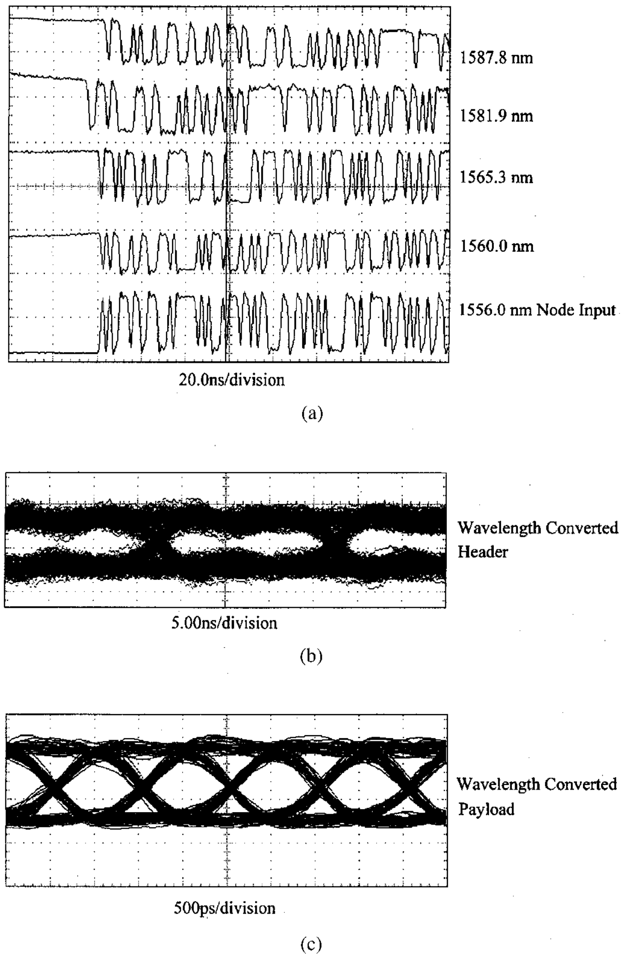

Fig. 3. (a) Wavelength conversion of original payload (lower trace) to four different wavelengths (1587.8 nm, 1581.9 nm, 1565.3 nm, and 1560 nm from top down). (b) Eye diagram of wavelength converted demodulated header. (c) Eye diagram of wavelength converted baseband.

nm due to the shorter tuning time between these adjacent wavelengths. The widths of the wavelength converted packets are broader than that of the input packets because the tunable laser is set for the entire packet length including the guard time. Following wavelength conversion, pattern inversion results from the cross gain modulation technique and the guard band filled with zeros is converted to ones. Pattern inversion due to wavelength conversion by cross gain modulation is undesirable for cascadability and future work will involve using a cross phase modulation wavelength conversion technique which will not invert the data or the guard band. Fig. 2(b) illustrates correct routing at the local switch modulator, with the input payload bits at the top, the modulator control signal in the middle, and the routed packets in the lower trace.

Demonstration of wavelength conversion of the baseband payload to the four output wavelengths is illustrated in Fig. 3(a). The traces are from separate measurement times, but have been stored and shifted to fit on a single oscilloscope output. The node input trace was from a packet destined for conversion to 1560 nm. The inputs that resulted in the other output wavelengths are not shown. Eye diagrams of wavelength converted payload and demodulated header are shown in Fig. 3(b) and (c), respectively. The modulation depth of the header was kept to a minimum to reserve as much optical power as possible for the payload as well as to minimize distortion of the subcarrier. The tradeoff between the payload and the header modulation depth was not optimized. Also, the electronic amplifiers used for header recovery introduced an undesirable level of noise into the header recovery process. The signal-to-noise ratio (SNR) for the wavelength converted signal will have to be optimized to cascade this operation. An alternative to converting the subcarrier header is to replace the subcarrier coded header all-optically to improve the header SNR at each node [8].

We have demonstrated a routing node for an all-optical multihop wavelength-routed packet switched network. The node utilizes switching in wavelength, temporal and spatial dimensions to provide connectivity between five wavelengths and three space ports. Subcarrier multiplexing was used to reduce the amount of optical power needed for header detection while simultaneously allowing conventional electronics to perform routing decisions for high-bit-rate packet payloads. The routing algorithm was chosen to provide operation that is compatible with arrayed waveguide WDM devices. Simultaneous wavelength conversion of the baseband payload and the subcarrier multiplexed header was also demonstrated. Finally, a novel fast tunable laser was employed to provide switching over a 40 nm range at the packet rate. Future work will involve the experimental demonstration of multihop operation as well as the use of an optical clock distribution scheme. Noninverting and SNR enhancing wavelength converting techniques are under investigation for integration into this node.

REFERENCES

[1] C. A. Brackett, A. S. Acampora, J. Sweitzer, G. Tangonan, M. T. Smith, W. Lennon, K. C. Wang, and R. H. Hobbs, "A scalable multiwavelength multihop optical network: A proposal for research on all-optical networks," *IEEE J. Lightwave Technol.*, vol. 11, pp. 736–753, May/June 1993.

[2] C. Dragone, "An $n \times n$ optical multiplexer using a planar arrangement of two star couplers," *IEEE Photon. Technol. Lett.*, vol. 3, pp. 812–815, Sept. 1991.

[3] A. Budman, E. Eichen, J. Schlafer, R. Olshansky, and F. McAleavey, "Multigigabit optical packet switch for self-routing networks with subcarrier addressing," in *Conference on Optical Fibers and Communications*, San Jose, CA, 1992, pp. 90–91.

[4] P. Poggiolini and S. Benedetto, "Performance analysis of multiple subcarrier encoding of packet headers in quasiall-optical WDM networks," *IEEE Photon. Technol. Lett.*, vol. 6, pp. 112–114, Jan. 1994.

[5] C.-L. Lu, D. J. B. Sabido, P. Poggiolini, R. T. Hofmeister, and L. G. Kazovsky, "CORD—a WDMA optical network: Subcarrier-based signaling and control scheme," *IEEE Photon. Technol. Lett.*, vol. 7, pp. 555–557, May 1995.

[6] C. Joergensen, T. Durhuus, B. Kikkelsen, R. J. Pedersen, K. E. Stubkjaer, P. Doussierre, G. Garabedian, C. Graver, E. Derouin, T. Fillion, D. Leclerc, and M. Klenk, "Efficient wavelength conversion at 10 gb/s in a polarization-insensitive, simple configuration," in *Proc. Conf. Optical Fibers and Commun.*, Feb. 1994, pp. 247–248.

[7] P. J. Rigole, S. Nillsson, L. Backbom, T. Klinga, J. Wallin, B. Stalnacke, E. Berglind, and B. Stoltz, "114 nm wavelength tuning rande of a vertical grating assisted codirectional coupler laser with a super structure grating distirbuted bragg reflector," *IEEE Photon. Technol. Lett.*, vol. 7, pp. 697–699, July 1995.

[8] M. Vaughn, A. Wang, and D. J. Blumenthal, "Simultaneous all-optical wavelength conversion of base-band payload and removal/replacement of subcarrier multiplexed headers," in *Tech. Dig. Conf. Optical Fibers and Commun. OFC '96*, San Jose, CA, Feb. 1996, pp. 128–129.